Improved Detection Probability of a Radar Target in the Presence of Multipath with Prior Knowledge of the Environment

Harun Taha Hayvaci*, Antonio De Maio†, Danilo Erricolo*

Email: hharun@ece.uic.edu, ademaio@unina.it, erricolo@uic.edu

*Department of Electrical and Computer Engineering

University of Illinois at Chicago

Chicago, USA

† Department of Biomedical, Electronic and Telecommunications Engineering

University of Naples "Federico II"

Napoli, Italy

Abstract

A new method to address radar target detection problems in multipath environments is considered. The novelty of the proposed method is that it exploits prior knowledge on the environment and combines it with ray-tracing electromagnetic modeling to determine some information about the possible multipath structure. This information is used to separate the environment into different regions based upon the behavior of the multipath components. Specifically, as a case study, we consider a radar and a target in the presence of a perfectly reflecting planar surface. For this environment, three regions are determined based upon the amount of overlap among the multipath components. For each region, receivers are designed exploiting the multipath structure. Thus, a different viewpoint to analyze radar detection problems is suggested. The two main results are the improvement in the target probability of detection, by properly accounting for the multipath, and *a priori* determination of the best performing detector based upon the location of the target and the available signal-to-noise ratio.

I. Introduction

This work is focused on improving the probability of detection of a radar target by taking advantage of prior knowledge of the radar-target environment and devising appropriate detectors based upon the region where the target is located. The improvement is computed with respect to a conventional detection problem based on a model of the return signal that accounts only for the direct signal from the target.

Radar detection problems are still challenging in all environments where multipath effects are present, notwithstanding the fact that they have been widely studied through advanced electromagnetic (EM) modeling [1], [2]. One approach to deal with multipath problems is to take the advantage of diversity [3]. In addition, with adaptive radars it has been well understood

that prior knowledge of the environment and its effective parameters may be used to enhance the detection, estimation and tracking performance of radar systems, *e.g.* [4]–[9], and references therein. Recently, with the development of advanced and computationally efficient EM tools, EM propagation models and simulations are being incorporated into radar and sensing problems as well, *e.g.* [10], [11]. Along these lines, this work investigates the problem of target detection in a multipath environment. Our work considers diverse receiving strategies by exploiting prior knowledge of the radar-target environment through advanced EM modeling of the corresponding multipath structure.

This article is organized as in the following. First, we consider a basic case study to show how to conduct an electromagnetic analysis that takes the advantage of prior knowledge of the environment where the radar operates. As a result, we obtain the propagation time of each multipath component. Then, the propagation time information is used to partition the environment into regions where diverse receiving strategies are applied. The criterion to determine the regions is the amount of overlap, in the time-domain, of the multipath components of the received signal. The amount of overlap depends on the environment, the location of radar and target, and the duration of the transmitted pulse. Accordingly, the general received signal model is specialized within each region to account for the presence of significant overlap or its absence. Then, within each region, a different receiver is devised thus justifying the statement of diverse receiving strategies. Neyman-Pearson tests (NP) as optimum detectors, and Generalized Likelihood Ratio Tests (GLRT) as sub-optimum detectors are devised for each region.

There are two main contributions in this article. First, it is possible to improve the probability of detection when the multipath components are distinguishable, compared to a conventional detector that does not take multipath information into account. A qualitative analysis is provided for the improvement in the target probability of detection via multipath exploitation when the multipath components are distinguishable and partially overlap in the time-domain. Second, it is possible to design detectors that have the best performance based upon prior knowledge of the region where the target is located.

Preliminary results were presented in [18]–[20].

II. Multipath Model and Time-Delay Analysis

We examine the case study shown in Fig. 1 because it contains only a few parameters and it has the advantage of allowing for an analytic discussion of this detection problem. This is a 2D geometry, where the origin of the cartesian coordinate system is the location of the radar and the target is located in a vertical plane at (x_t, z_t).

A high frequency ray-tracing electromagnetic analysis of this geometry provides the following expression for the received signal of interest with a two-ray model

$$r_s(t) = \alpha_1(t)s(t-\tau_1) + \alpha_2(t)s(t-\tau_2), \tag{1}$$

where $r_s(t)$ and $s(t)$ are the baseband equivalents of the received signal of interest and transmitted signal respectively, $\alpha_1(t)$ and $\alpha_2(t)$ are complex parameters accounting for propagation and scattering effects, and τ_1 and τ_2 are time delays along the corresponding propagation paths. Although there would be three propagation paths and three time delays for the geometry depicted in Fig. 1, a two-ray model is sufficient to show the potential improvement of multipath exploitation. We assume a planar surface that provides only a specular reflection. For applications related to modeling the reflection from rough surfaces,

one would have to add a contribution from diffuse reflection mechanisms. These mechanisms have been investigated, for example, in [21], [22].

The electromagnetic ray-tracing analysis of the environment is always capable to predict the time-delays associated with each multipath component as shown, for example, in [23]–[25]. The time-delays and associated time-delay differences for all possible locations of the target can be computed with the geometrical parameters, *i.e.* x_t, z_t, and h_s, as shown in [18]. Assuming a pulse duration T, we define the regions where multipath components overlap, when $|\tau_2 - \tau_1| \leq T$, and the regions where the multipath components are distinguishable, when $|\tau_2 - \tau_1| > T$. An example of partitioning the multipath environment for $T = 10$ ns can be found in [18]. This prompts us to diversify the detection strategy within each region.

III. Formulation of the Detection Problem

The signal representations and corresponding hypothesis testing problems for each region are derived. Exploiting the useful received signal model given in (1), we assume

$$s(t) = \begin{cases} \frac{1}{\sqrt{T}} & 0 \leq t \leq T \\ 0 & \text{elsewhere} \end{cases}, \tag{2}$$

$$\alpha_1(t) = \begin{cases} \text{unknown} & \tau_1 \leq t \leq T + \tau_1 \\ 0 & \text{elsewhere} \end{cases}, \tag{3}$$

$$\alpha_2(t) = \begin{cases} \text{unknown} & \tau_2 \leq t \leq T + \tau_2 \\ 0 & \text{elsewhere} \end{cases}. \tag{4}$$

The pulse duration T is assumed to be small compared to the coherence time of the target, so that $\alpha_1(t)$ and $\alpha_2(t)$ can be approximated with two unknown complex deterministic constants α_1 and α_2, respectively.

Region I is defined by $|\tau_2 - \tau_1| \ll T$ and the received signal (under the hypothesis where target is present) is represented as

$$\begin{aligned} r(t) &= \alpha_1 s(t - \tau_1) + \alpha_2 s(t - \tau_2) + w(t) \\ &\simeq \alpha s(t - \tau_1) + w(t) \end{aligned} \tag{5}$$

without any significant loss of the received energy. α is an unknown complex deterministic parameter, $r(t)$ and $w(t)$ are the baseband equivalents of the received signal and noise, respectively. Accordingly, the detection problem can be formulated as the following hypothesis test

$$\begin{aligned} H_0&: \quad r(t) = w(t) \\ H_1&: \quad r(t) = \alpha s(t - \tau_1) + w(t) \end{aligned} \qquad t \in [\tau_1, T + \tau_1] \tag{6}$$

where $[\tau_1, T + \tau_1]$ is the observation interval.

Region II is defined by $|\tau_2 - \tau_1| \geq T$; hence multipath components are resolvable in time-domain and exploited in the

receiver. Accordingly, the detection problem can be formulated as

$$\begin{aligned} H_0: &\quad r(t) = w(t) \\ H_1: &\quad r(t) = \alpha_1 s(t-\tau_1) + \alpha_2 s(t-\tau_2) + w(t) \end{aligned} \tag{7}$$

where $t \in [\tau_1,\ T+\tau_2]$, which is the observation interval. Since $|\tau_2 - \ \tau_1| \geq \ T,\ \ s(t-\tau_1)$ and $s(t-\tau_2)$ are orthogonal signals, we have $\int_{-\infty}^{\infty} s(t-\tau_1)\ s^*(t-\tau_2)\ dt = 0$, where $(.)^*$ is the complex conjugate operator.

The likelihood ratio test in both regions can be written as

$$\Lambda[r(t)|\mathbf{\Theta}] = \frac{p_{r(t)|\mathbf{\Theta},H_1}\left(r(t)|\mathbf{\Theta},H_1\right)}{p_{r(t)|H_0}\left(r(t)|H_0\right)}, \tag{8}$$

where $p_{r(t)|\mathbf{\Theta},H_1}\left(r(t)|\mathbf{\Theta},H_1\right)$ and $p_{r(t)|H_0}\left(r(t)|H_0\right)$ are the likelihood functions, $\mathbf{\Theta}$ is the vector of unknown parameters, *i.e.*

$$\mathbf{\Theta} = \begin{cases} [\alpha] & \text{in Region I} \\ [\alpha_1, \alpha_2]^T & \text{in Region II.} \end{cases} \tag{9}$$

In the Transition Region, the time-delay difference is shorter than the transmitted pulse duration T but not as short as in Region I, *i.e* $|\tau_2 - \tau_1| < T$. Thus multipath return signals along different paths are neither highly clumped nor resolvable in time-domain. The received signal in the Transition Region under the hypotheses H_0 and H_1 are the same as (7) in Region II. However, $s(t-\tau_1)$ and $s(t-\tau_2)$ are no longer orthogonal signals since $|\tau_2 - \ \tau_1| < \ T$ and we have $\int_{-\infty}^{\infty} s(t-\tau_1)\ s^*(t-\tau_2)\ dt = \rho$, which is a real number in this particular scenario.

IV. Optimum and Sub-Optimum Detectors

The optimum and sub-optimum detectors are sought assuming that $w(t)$ is a zero-mean complex circular white Gaussian noise (CWGN), with known power spectral density (PSD) σ^2. A conventional approach, based on projecting the received waveform along the first M functions of an orthonormal basis and letting M diverge, is adopted. Precisely, having chosen the basis $ß = \{\phi_i(t)\}_{i=1}^{\infty}$, the received signal is represented by components $R_i = \langle r(t), \phi_i(t)\rangle$, where $\langle \cdot, \cdot \rangle$ denotes the scalar product in the space of finite energy signals. Then the likelihood ratio (8) can be written as

$$\begin{aligned} \Lambda[r(t)|\mathbf{\Theta}] &= \lim_{M\to\infty} \Lambda_M[r_M(t)|\mathbf{\Theta}] \\ &= \lim_{M\to\infty} \frac{p_{\mathbf{R_M}|\mathbf{\Theta},H_1}\left(\mathbf{R_M}|\mathbf{\Theta},H_1\right)}{p_{\mathbf{R_M}|H_0}\left(\mathbf{R_M}|H_0\right)}, \end{aligned} \tag{10}$$

where $\mathbf{R_M}$ is the vector containing the first M coefficients of the received signal waveform and $r_M(t)$ is the projection of the received signal on the subspace spanned by the first M functions of the basis, [26], [27]. Since we have zero mean CWGN with PSD σ^2, R_i is complex Gaussian with (i) μ_i mean and variance σ^2 under H_1 hypothesis; and (ii) zero mean and variance σ^2 under H_0 hypothesis. Thus, the likelihood function is readily found as

$$\lim_{M\to\infty} \Lambda_M[r_M(t)|\mathbf{\Theta}] = \lim_{M\to\infty} \frac{\prod_{i=1}^{M} \frac{1}{\pi\sigma^2} \exp\left(-\frac{|R_i-\mu_i|^2}{\sigma^2}\right)}{\prod_{i=1}^{M} \frac{1}{\pi\sigma^2} \exp\left(-\frac{|R_i|^2}{\sigma^2}\right)}, \tag{11}$$

where μ_i is the expected value of R_i.

First we assume that $\mathbf{\Theta}$ is a known set of parameters in order to deduct the optimal detector. Although this hypothesis is not realistic for real world radar and sonar problems, it provides an upper bound for any receiver operating under the same signal model. It is also important to observe whether a Uniformly Most Powerful (UMP) test exists or does not exist.

A. Region I: Multipath returns are highly clumped

We formulate the detection problem, based on (6), as

$$\begin{aligned} H_1\text{:}\quad & R_i = \langle r(t), \phi_i(t) \rangle = \begin{cases} \alpha + W_1, & i = 1 \\ W_i, & i > 1 \end{cases} \\ H_0\text{:}\quad & R_i = \langle r(t), \phi_i(t) \rangle = W_i \end{aligned} \tag{12}$$

where $\phi_1(t) = s(t - \tau_1)$, so that $\mu_1 = \alpha$ and $\mu_{i \neq 1} = 0$. By evaluating the likelihood ratio (11) with the knowledge of $\mathbf{\Theta}$ and taking the logarithm, one obtains the log-likelihood ratio, up to a constant and irrelevant factor, as

$$\ln \Lambda[r(t)|\mathbf{\Theta}] = \frac{|R_1|^2 - |R_1 - \alpha|^2}{\sigma^2}. \tag{13}$$

Then the corresponding NP test, which we call NP1, is given as, [27], [28],

$$\Re \left\{ \sqrt{\frac{2}{\sigma^2}} \alpha^* R_1 \right\} \underset{H_0}{\overset{H_1}{\gtrless}} \gamma_1, \tag{14}$$

where $\Re\{.\}$ is the real part operator and γ_1 is the threshold. This is a hypothetical test with the perfect measurement or the knowledge of α in the detector. Although (14) is not a UMP test with respect to α, it provides an upper bound to the performance of any practically implementable detector. GLRT is a common technique to devise detectors with unknown parameters, particularly when no UMP test exists. GLRT uses the maximum likelihood estimates (MLE) of unknown parameters under both hypotheses in the likelihood ratio [27], [28].

Thus, the corresponding GLRT detector with respect to α is given as

$$\frac{2}{\sigma^2} |R_1|^2 \underset{H_0}{\overset{H_1}{\gtrless}} \gamma_1', \tag{15}$$

which we call GLRT1. It can be realized with a standard matched-filter followed by square modulus [27], [28].

B. Region II: Multipath returns are entirely resolvable

The basis functions $ß = \{\phi_i(t)\}_{i=1}^{M}$ are selected as

$$\begin{aligned} \phi_1(t) &= s(t - \tau_1) \quad \tau_1 \leq t \leq T + \tau_1 \\ \phi_2(t) &= s(t - \tau_2) \quad \tau_2 \leq t \leq T + \tau_2 \end{aligned} \tag{16}$$

so that the detection problem for Region II becomes

$$\begin{aligned} H_1\text{:}\quad & R_i = \langle r(t), \phi_i(t) \rangle = \begin{cases} \alpha_1 + W_1, & i = 1 \\ \alpha_2 + W_2, & i = 2 \\ W_i, & i > 2 \end{cases} \\ H_0\text{:}\quad & R_i = \langle r(t), \phi_i(t) \rangle = W_i. \end{aligned} \tag{17}$$

By evaluating the likelihood ratio (11) in Region II with the knowledge of $\mathbf{\Theta}$ and taking the logarithm, we obtain the corresponding log-likelihood ratio, up to a constant and irrelevant factor, as

$$\begin{aligned} \ln \Lambda[r(t)|\mathbf{\Theta}] = & - \frac{|R_1 - \alpha_1|^2 + |R_2 - \alpha_2|^2}{\sigma^2} \\ & + \frac{|R_1|^2 + |R_1|^2}{\sigma^2}. \end{aligned} \tag{18}$$

After simple manipulations, the log-likelihood ratio test, which we call NP2, is derived as

$$\Re \left\{ \sqrt{\frac{2}{\sigma^2}} \left[\alpha_1^* R_1 + \alpha_2^* R_2 \right] \right\} \underset{H_0}{\overset{H_1}{\gtrless}} \gamma_2, \tag{19}$$

where γ_2 is the threshold. This is a hypothetical test with the perfect measurement or the knowledge of α_1 and α_2 in the detector. Additionally, it is not a UMP test with respect to α_1 and α_2, thus GLRT approach is applied next. GLRT substitutes the unknown signal parameters with $\hat{\mathbf{\Theta}} = [\hat{\alpha}_1, \hat{\alpha}_2]^T$ in the log-likelihood ratio (18). $\hat{\mathbf{\Theta}}$ is the MLE of $\mathbf{\Theta}$ under H_1 that maximizes the corresponding likelihood function, [28], [29], *i.e.*

$$\hat{\mathbf{\Theta}} = [\hat{\alpha}_1, \hat{\alpha}_2]^T = [R_1, R_2]^T. \tag{20}$$

The corresponding GLRT, which we call GLRT2, can be written as

$$\frac{2}{\sigma^2} \left[|R_1|^2 + |R_2|^2 \right] \underset{H_0}{\overset{H_1}{\gtrless}} \gamma_2'. \tag{21}$$

C. Transition Region

For this region, no particular detector is devised since there is no stable structure of the multipath. Therefore, we analyze the performance of NP2 and GLRT2, which exploit multipath, in comparison with NP1 and GLRT1, which exploit the direct return path only.

V. Performance Assessment

In this section, we assess the performance of the proposed detectors GLRT2 (21) and NP2 (19), which exploit multipath, as well as the conventional detectors GLRT1 (15) and NP1 (14), which only account for the direct return signals.

Before discussing the performance of these detectors, we need to define the corresponding probabilities of false alarm and detection.

A. Probabilities of False Alarm and Detection

The probability of false alarm of NP1 is

$$P_{FA_{\mathbf{NP1}}} = Q\left(\frac{\gamma_1}{\sqrt{|\alpha|^2}}\right) \tag{22}$$

yielding the threshold

$$\gamma_1 = |\alpha| Q^{-1}\left(P_{FA_{\mathbf{NP1}}}\right), \tag{23}$$

and the corresponding probability of detection

$$P_{D_{\mathbf{NP1}}} = Q\left(Q^{-1}(P_{FA_{\mathbf{NP1}}}) - \sqrt{\frac{|\alpha|^2}{\sigma^2/2}}\right), \tag{24}$$

where $Q(.)$ and $Q^{-1}(.)$ are the Complementary Cumulative Distribution Function (CCDF), and inverse CCDF of a standard Gaussian random variable, respectively, pp. 20-28 of [28]. The probability of false alarm of GLRT1 is

$$P_{FA_{\mathbf{GLRT1}}} = Q_{\chi_2^2}\left(\gamma_1'\right) \tag{25}$$

yielding the threshold

$$\gamma_1' = Q_{\chi_2^2}^{-1}\left(P_{FA_{\mathbf{GLRT1}}}\right) \tag{26}$$

and the corresponding probability of detection,

$$P_{D_{\mathbf{GLRT1}}} = Q_{\chi_2'^2(\lambda)}\left(Q_{\chi_2^2}^{-1}\left(P_{FA_{\mathbf{GLRT1}}}\right)\right), \tag{27}$$

where $Q_{\chi_2^2}(.)$ and $Q_{\chi_2'^2(\lambda)}(.)$ are the CCDF of a χ_2^2, and a $\chi_2'^2(\lambda)$ where non-centrality parameter $\lambda = 2|\alpha|^2/\sigma^2$, respectively, pp. 20-28 of [28].

The test statistics of NP2 under both hypotheses are Gaussian, thus the probability of false alarm is obtained as

$$P_{FA_{\mathbf{NP2}}} = Q\left(\frac{\gamma_2}{\sqrt{(|\alpha_1|^2 + |\alpha_2|^2)}}\right) \tag{28}$$

yielding the threshold,

$$\gamma_2 = Q^{-1}(P_{FA_{\mathbf{NP2}}})\sqrt{|\alpha_1|^2 + |\alpha_2|^2} \tag{29}$$

and the probability of detection,

$$P_{D_{\mathbf{NP2}}} = Q\left(Q^{-1}(P_{FA_{\mathbf{NP2}}}) - \sqrt{\frac{|\alpha_1|^2 + |\alpha_2|^2}{\sigma^2/2}}\right). \tag{30}$$

When we consider GLRT2 under H_0, the test statistics is the product between $2/\sigma^2$ and the sum of the square magnitudes of two complex circular Gaussian variables with zero mean and variance σ^2. It can be shown that this test statistics has χ_4^2

distribution. Consequently, the probability of false alarm can be written as

$$P_{FA_{\mathbf{GLRT2}}} = Q_{\chi_4^2}\left(\gamma_2'\right) \tag{31}$$

yielding the threshold,

$$\gamma_2' = Q_{\chi_4^2}^{-1}\left(P_{FA_{\mathbf{GLRT2}}}\right). \tag{32}$$

However, when we consider GLRT2 under H_1, the test statistics is the product between $2/\sigma^2$ and the sum of the square magnitudes of two complex circular Gaussian random variables with non-zero mean and variance σ^2. Again, it can be shown that the test statistics has a $\chi_4'^2(\lambda_{12})$ distribution, [28]. As a consequence, the probability of detection of GLRT2 can be written as

$$P_{D_{\mathbf{GLRT2}}} = Q_{\chi_4'^2(\lambda_{12})}\left(Q_{\chi_4^2}^{-1}\left(P_{FA_{\mathbf{GLRT2}}}\right)\right) \tag{33}$$

where

$$\lambda_{12} = \frac{2}{\sigma^2}(|\alpha_1|^2 + |\alpha_2|^2) = \lambda_1 + \lambda_2 \tag{34}$$

where $\lambda_1 = 2|\alpha_1|^2/\sigma^2$ and $\lambda_2 = 2|\alpha_2|^2/\sigma^2$. It is also important to note that $\lambda = \lambda_1$, *i.e.* $\alpha = \alpha_1$, in Region II.

In the Transition Region, we explore the use of two detection strategies. Accordingly, we first determine their statistical characterizations. Then the corresponding probabilities of false alarm and detection are provided.

The probabilities of false alarm of NP1 and GLRT1 in this region are the same as (22) and (25), respectively, but the probabilities of detection are different and obtained as

$$P_{D_{\mathbf{NP1_T}}} = Q\left(Q^{-1}\left(P_{FA_{\mathbf{NP1}}}\right) - \frac{|\alpha_1|^2 + \Re\{\rho\alpha_1^*\alpha_2\}}{\sqrt{|\alpha_1|^2\sigma^2/2}}\right) \tag{35}$$

and

$$P_{D_{\mathbf{GLRT1_T}}} = Q_{\chi_2'^2(\lambda_T)}\left(Q_{\chi_2^2}^{-1}\left(P_{FA_{\mathbf{GLRT1}}}\right)\right) \tag{36}$$

where

$$\lambda_T = \frac{2}{\sigma^2}|\alpha_1 + \rho\alpha_2|^2. \tag{37}$$

The probabilities of false alarm and detection of NP2 (19) and GLRT2 (21) in the Transition Region, are not the same as (28), (30), (31) and (33), respectively. The covariance of the random variables R_1 and R_2 in detectors has to be taken into account to characterize the probability distribution functions. The covariance of R_1 and R_2 is readily found by $COV\left[R_1, R_2^*\right] = \rho\sigma^2$.

The probabilities of false alarm and detection of NP2 are obtained respectively as

$$P_{FA_{\mathbf{NP2_T}}} = Q\left(\frac{\gamma_2}{\sqrt{|\alpha_1|^2 + |\alpha_2|^2 + 2\rho\Re\{\alpha_1\alpha_2^*\}}}\right), \tag{38}$$

$$P_{D_{\mathbf{NP2_T}}} = Q\left(Q^{-1}(P_{FA_{\mathbf{NP2_T}}}) - \sqrt{\frac{|\alpha_1|^2 + |\alpha_2|^2 + 2\rho\Re\{\alpha_1\alpha_2^*\}}{\sigma^2/2}}\right). \tag{39}$$

The test statistics of GLRT2 is the sum of square magnitudes of two correlated complex circular Gaussian random variables R_1 and R_2 with the covariance matrix $\mathbf{C_R}$, where

$$\mathbf{C_R} = \sigma^2 \begin{bmatrix} 1 & \rho \\ \rho & 1 \end{bmatrix}, \tag{40}$$

by letting $\mathbf{R} = [R_1, R_2]^T$. We represent (21) in the Transition Region with two statistically independent random variables, obtaining

$$[(1+\rho)R_s + (1-\rho)R_d] \underset{H_0}{\overset{H_1}{\gtrless}} \gamma_2', \tag{41}$$

where $R_s = \frac{|R_1+R_2|^2}{\sigma^2(1+\rho)}$, and $R_d = \frac{|R_1-R_2|^2}{\sigma^2(1-\rho)}$. They are two independent random variables that have χ_2^2 distribution under H_0, $\chi_2'^2(\lambda_s)$ and $\chi_2'^2(\lambda_d)$ distributions, respectively, under H_1, where

$$\lambda_s = \frac{(1+\rho)|\alpha_1+\alpha_2|^2}{\sigma^2} \tag{42}$$

$$\lambda_d = \frac{(1-\rho)|\alpha_1-\alpha_2|^2}{\sigma^2} \tag{43}$$

so that the test statistics of (41) is

$$T_R = (1+\rho)R_s + (1-\rho)R_d. \tag{44}$$

Now we can compute the probabilities of false alarm and detection for (41). The probability of false alarm can be obtained as

$$P_{FA_{\mathbf{GLRT2_T}}} = P\left[T_R|H_0 > \gamma_2'\right] = P\left[\sum_{k=1}^{2} c_k\chi_2^2 > \gamma_2'\right], \tag{45}$$

where $T_R|H_0$ is the test statistics of (41) under H_0, $c_1 = 1+\rho$, and $c_2 = 1-\rho$ are the constant coefficients of two independent χ_2^2 random variables. By the theorem for finite linear combinations of independent central χ^2 probabilities (see Appendix-A, [31]) we obtain the probability of false alarm explicitly as

$$\begin{aligned} P_{FA_{\mathbf{GLRT2_T}}} &= F_1(1+\rho, \gamma_2') + F_2(1-\rho, \gamma_2') \\ &= \frac{1+\rho}{2\rho}\exp\left\{-\frac{\gamma_2'}{2(1+\rho)}\right\} - \frac{1-\rho}{2\rho}\exp\left\{-\frac{\gamma_2'}{2(1-\rho)}\right\}. \end{aligned} \tag{46}$$

In a similar manner, the probability of detection can be obtained as

$$P_{D_{\mathbf{GLRT2_T}}} = P\left[T_R|H_1 > \gamma_2'\right] = P\left[\sum_{k=1}^{2} c_k\chi_2^2(\lambda_k') > \gamma_2'\right], \tag{47}$$

where $T_R|H_1$ is the test statistics of (41) under H_1, $c_1 = 1+\rho$, $c_2 = 1-\rho$ are the constant coefficients of two independent $\chi_2'^2(\lambda_k')$ distributions with non-centrality parameters $\lambda_1' = \lambda_s$ and $\lambda_2' = \lambda_d$, which are given by (42) and (43), respectively.

The cumulative distribution function of the sum of M independent $\chi^2_{v_k}(\lambda_k)$ with different coefficients is given in Appendix-B, [31]. As a consequence, the probability of detection is obtained in an analytic form as

$$P_{D_{\mathbf{GLRT2_T}}} = \frac{1}{2} + \frac{1}{\pi}\int_0^\infty \frac{\sin\theta(u)}{u\rho(u)}du, \tag{48}$$

where

$$\theta(u) = \frac{1}{2}\sum_{k=1}^{2}\left[2\tan^{-1}(c_k u) + \lambda_k c_k u(1+c_k^2u^2)^{-1}\right] - \frac{1}{2}\gamma_2 u,$$
$$\rho(u) = \prod_{k=1}^{2}(1+c_k^2u^2)^{\frac{1}{2}}\exp\left\{\frac{1}{2}\sum_{k=1}^{2}\frac{\lambda_k(c_k u)^2}{(1+c_k^2u^2)}\right\}.$$

B. Simulation Results and Discussion

Now that the appropriate probabilities for the detectors in consideration have been introduced, we are ready to compare the performance of these detectors. Since GLRT1 and GLRT2 are not optimum detectors, first it is necessary to assess the performance loss with respect to NP1 and NP2 which assume perfect knowledge of signal parameters.

This analysis was provided in [18] by the same authors of this article and the results are briefly summarized in the following paragraph.

The degradation in the detection performance of the proposed GLRT2 with respect to NP2 was found less than 2 dB in signal-to-noise ratio (SNR) for a low probability of false alarm, *i.e.* $P_{FA} = 10^{-3}$. For the convenience of making a comparison, the conventional GLRT1 and NP1 were tested under the same multipath environment as GLRT2 and NP2. The degradation in the conventional case was found to be 1 dB in SNR for the same $P_{FA} = 10^{-3}$. The fact that the degradation between NP1 and GLRT1 is smaller than the degradation between GLRT2 and NP2 is expected, since GLRT2 requires the estimation of two unknown parameters. In practice, imperfect prior knowledge on τ_1 and τ_2 can lead to a further performance loss.

The primary goal of this paper is to show that diverse receiving strategies can be utilized in challenging multipath radar-target environments for better detection performances. In a conventional approach, GLRT1 would be applied for all regions of a radar-target geometry such as those described in this article. In the proposed approach, NP1 and GLRT1 are devised as optimum and sub-optimum detectors in Region I only, whereas NP2 and GLRT2 are devised as optimum and sub-optimum detectors in Region II. Thus it is important to assess the performance improvement of (i) NP2 relative to NP1; and, (ii) GLRT2 relative to GLRT1, particularly when multipath returns are resolvable as in Region II, and partially overlap in time-domain as in the Transition Region.

1) Performance Comparison in Region II: The performance of the detectors in this region depends upon the ratio λ_2/λ_1. Therefore we perform the comparison of the two detection strategies based upon the various values of the ratio λ_2/λ_1.

In Fig. 3 we compare NP2 and NP1 with respect to the SNR value of the direct return path, namely SNR $= 10\log_{10} 2|\alpha_1|^2/\sigma^2$. Both receivers are tested under the same multipath environment. Despite of NP1, NP2 exploits the reflected return path which is assumed to be proportional to the direct path strength. Thus, Fig. 3 assesses the quantitative measure of the optimal performance improvement of the receiver that exploits multipath compared to the traditional receiver that relies on the direct return path only. We observe that (i) the performance of NP2 is always superior to the one of NP1 that the improvement amount depends

upon the ratio λ_2/λ_1 between the multipath returns; and, (ii) their performance merges when the second return path is weak compared to the direct return path, *i.e.* $\lambda_2 = 0.01\lambda_1$.

In Fig. 2 we compare sub-optimum receivers GLRT2 and GLRT1, under the same multipath environment, with respect to the SNR value of the direct return path. In general, the performance of GLRT2 is also superior to the one of GLRT1, depending upon the SNR value of the multipath returns. However, GLRT1 outperforms GLRT2 when the second return path is weak compared to the direct return path. This is well understandable because GLRT2 has an extra cost of estimating a second unknown parameter which requires a certain level of SNR.

In Fig. 4 we present another comparison for a lower value of the probability of false alarm, in order to emphasize that GLRT2 outperforms GLRT1 unless $\lambda_2 \ll \lambda_1$. One can observe that for lower values of the probability of false alarm it is even more evident that GLRT2 outperforms GLRT1.

2) Performance Comparison in the Transition Region: The performance in the Transition Region depends upon the degree of overlap of the multipath returns. Therefore we perform a comparison of the two detection strategies based upon the correlation coefficient of the multipath returns. In the following analysis we assume $|\alpha_1| = |\alpha_2|$, so that direct and reflected path returns have same SNR value, *i.e.* $\lambda_1 = \lambda_2$.

First we compare the two detectors assuming very low and very high correlation of multipath signal returns: (i) $\rho = 0.01$ and (ii) $\rho = 0.99$. We observe that (1) when the correlation coefficient is very low the signals are essentially distinguishable and the probability of detection behaves similar to what was found in Region II as shown in Fig. 5(a); and, (2) when the correlation coefficient is very high then the signals are essentially highly clumped and the probability of detection behaves similar to what was found in Region I as shown in Fig. 5(b). In fact, $\rho = 0.01$ and $\rho = 0.99$ are not belong to Transition Region but Region II and Region I, respectively. However, it is necessary with Fig. 5 to validate the expressions of the probabilities of false alarm and detection in the Transition Region, *i.e.* (36), (46) and (48).

Second we present the performance of the detectors when $\rho = 0.5$. Our results indicate that the performance of the GLRT2 detector depends on the phase difference between the first and second returns, since the correlation of multipath signal returns are non-negligible. Thus, two extreme situations, in-phase and out-of-phase, are considered in Fig. 6(a) and Fig. 6(b), respectively. When α_1 and α_2 are in phase, the performance of GLRT2 is always superior to the one of GLRT1, while, when α_1 and α_2 are out-of-phase, the performance of GLRT2 is only superior to GLRT1 for SNR values above 5 dB. This occurs because GLRT2 is affected by the correlation coefficient since it accounts for two signals, while GLRT1 is independent of the correlation coefficient because it exploits the direct signal only.

Finally, the improvement in the target probability of detection of GLRT2 relative to GLRT1 at any hypothetical target location in the multipath environment is presented in Fig. 7. It is assumed that γ_2', which is the threshold for GLRT2, is fixed at $P_{FA_{\mathbf{GLRT2}}} = 10^{-5}$ by (32). However, $P_{FA_{\mathbf{GLRT2_T}}}$ varies across the Transition Region since it depends on ρ as shown in (46). In order to compare two detectors at the same level of P_{FA} we make $P_{FA_{\mathbf{GLRT1_T}}} = P_{FA_{\mathbf{GLRT2_T}}}$ across all regions by changing the threshold γ_1' of GLRT1. It is also assumed that $|\alpha_1| = |\alpha_2|$ and SNR $= 10\log_{10}(2|\alpha_1|^2/\sigma^2) = 12$ dB. Constructive and destructive effects of multipath is also shown in Fig. 7 in the sense of target probability of detection at a certain SNR level of multipath returns.

3) Performance Comparison in Region I: In Fig. 5(b) and Fig. 7 one can see that GLRT2 merges to GLRT1, in Region I.

VI. Conclusion

We considered the detection of a target by a radar in a multipath environment. We show that by taking advantage of the multipath it is possible, in general, to increase the probability of detection of the target, compared to a conventional detection problem based on a model of the return signal that accounts only for the direct signal return from the target.

Multipath is accounted for by leveraging on prior knowledge of the environment where the radar operates. Using this prior knowledge and electromagnetic high-frequency ray-tracing analysis, we can predict the time of arrival of each multipath return depending upon the assumed location of the target. In the case study considered, we show that the environment can be divided into three regions: (1) Region II where multipath components can be clearly distinguished and where the probability of detection is improved by properly accounting for the multipath; (2) Region I where multipath components cannot be distinguished and there is no possibility of improving the probability of detection; and, (3) the Transition Region where, depending upon the SNR of each individual component and the correlation coefficient of the multipath components, it is possible to improve upon a conventional detector. Thus, it is also shown here that diverse receiving strategies, which are optimum in the particular regions of the multipath environment, can be applied to exploit the best performing receivers.

This article provides a method to account for multipath as well as the quantitative analysis of the performance increase due to the multipath exploitation. The method was explained by referring to a basic case study scenario, however the approach is quite general and it could be extended to more complex environments.

Appendix

Suppose constant coefficients $c_1 > c_2 > \cdots > c_m > 0$ and $\gamma > 0$.

A. Finite Linear Combinations of Independent χ^2 Variables

$$P\left[\sum_{k=1}^{m} c_k \chi^2_{2v_k} \;>\; \gamma\right] = \sum_{k=1}^{m} \frac{1}{(v_k-1)!}\left[\frac{\partial^{v_k-1}}{\partial c^{v_k-1}} F_k(c,\gamma)\right]_{c=c_k} \tag{49}$$

where

$$F_k[c,\gamma] = c^{n-1}\exp\{-\gamma/(2c)\}\prod_{r=1,r\neq k}^{m}(c-c_r)^{-v_r}, \tag{50}$$

where $n = \sum_{k=1}^{m} v_k$.

B. Finite Linear Combinations of Independent $\chi^2_{v_k}(\lambda_k)$ Variables

$$P\left[\sum_{k=1}^{m} c_k \chi^2_{v_k}(\lambda_k) > \gamma\right] = \frac{1}{2} + \frac{1}{\pi}\int_0^{\infty} \frac{\sin\theta(u)}{u\rho(u)} du, \tag{51}$$

where

$$\theta(u) = \frac{1}{2}\sum_{k=1}^{m}\left[v_k \tan^{-1}(c_k u) + \lambda_k c_k u(1+c_k^2 u^2)^{-1}\right] - \frac{1}{2}\gamma u,$$
$$\rho(u) = \prod_{k=1}^{m}(1+c_k^2 u^2)^{\frac{1}{4}v_k} \exp\left\{\frac{1}{2}\sum_{k=1}^{m}\frac{\lambda_k (c_k u)^2}{(1+c_k^2 u^2)}\right\}. \tag{52}$$

REFERENCES

[1] M. I. Skolnik (Ed.), *Radar Handbook,* The McGraw-Hill Companies, 2008.

[2] F. E. Nathanson, J. P. Reilly, M. N. Cohen, *Radar Design Principles, Signal Processing and the Environment,* Mendham, New Jersey: Scitech Publishing, 1999.

[3] S. Benedetto and E. Biglieri, *Principles of Digital Transmission with Wireless Applications*, ch.13, New York: Kluwer Academic Publishers, 2002.

[4] F. C. Robey, D. R. Fuhrmann, E. J. Kelly, R. Nitzberg, "A CFAR adaptive matched filter detector, *IEEE Trans. Aerospace and Electronic Systems*, vol. 28, no. 1, pp. 208-216, Jan 1992.

[5] W. L. Melvin "Space-time adaptive radar performance in heterogenous clutter," *IEEE Trans. Aerospace and Electronic Systems*, vol. 36, no. 2, pp. 621-633, Apr. 2000.

[6] A. De Maio, A. Farina, M. Wicks, "KB-GLRT: exploiting knowledge of the clutter ridge in airborne radar, *Radar, Sonar & Navigation, IEE Proceedings*, vol. 152, no. 6, pp. 421- 428, 9 Dec. 2005.

[7] F. Gini (Ed.) "Knowledge-based systems for adaptive radar: Detection, tracking and classification," *IEEE Signal Processing Magazine*, vol. 23, no. 1, pp. 14-76, Jan. 2006.

[8] J. R. Guerci, and W. L. Melvin (Eds.) "Special section on knowledge-aided sensor signal and data processing," *IEEE Trans. Aerospace and Electronic Systems*, vol. 42, no. 3, pp. 983-1120, July 2006.

[9] A. De Maio, A. Farina, G. Foglia, "Design and experimental validation of knowledge-based constant false alarm rate detectors," *Radar, Sonar & Navigation, IET*, vol. 1, no. 4, pp. 308-316, Aug. 2007.

[10] T. Dogaru, A. Sullivan, C. Kenyon, C. Le, "Radar Signature Prediction for Sensing-through-the-Wall by Xpatch and AFDTD," *High Performance Computing Modernization Program Users Group Conference (HPCMP-UGC), 2009 DoD,* pp. 339-343, 15-18 June 2009.

[11] T. Dogaru, A. Sullivan, C. Le, C. Kenyon, , "Radar Signature Prediction for Sensing-Through-the-Wall by Xpatch and AFDTD - Part II," *High Performance Computing Modernization Program Users Group Conference (HPCMP-UGC), 2010 DoD,* pp. 401-406, 14-17 June 2010.

[12] J. L. Krolik, J. Farrell, A. Steinhardt, "Exploiting multipath propagation for GMTI in urban environments," *Radar Conference (RADAR), 2006 IEEE*, pp. 24-27, April 2006.

[13] B. Chakraborty, Y. Li, J. J. Zhang, T. Trueblood, A. Papandreou-Suppappola, D. Morrell, "Multipath exploitation with adaptive waveform design for tracking in urban terrain," *Acoustics Speech and Signal Processing (ICASSP), 2010 IEEE International Conference on*, pp. 3894-3897, 14-19 March 2010.

[14] S. Sen, A. Nehorai, "Adaptive OFDM Radar for Target Detection in Multipath Scenarios," *IEEE Trans. on Signal Processing,* vol. 59, no. 1, pp. 78-90, Jan. 2011.

[15] V. Krishnan, B. Yazici , "Synthetic aperture radar imaging exploiting multiple scattering," *Inverse Problems*, vol. 27, no. 5, 055004, May 2011.

[16] P. Setlur, M. G. Amin, F. Ahmad, "Multipath Model and Exploitation in Through-the-Wall and Urban Radar Sensing," *IEEE Trans. Geoscience and Remote Sensing,* vol. 49, no. 10, pp. 4021-4034, Oct. 2011.

[17] P. Setlur, G. E. Smith, F. Ahmad, M. G. Amin, "Target Localization with a Single Sensor via Multipath Exploitation," *IEEE Trans. Aerospace and Electronic Systems*, accepted for publication.

[18] H. T. Hayvaci, A. De Maio, D. Erricolo, "Diversity in receiving strategies based on time-delay analysis in the presence of multipath," *Radar Conference (RADAR), 2011 IEEE*, pp. 1040-1045, 23-27 May 2011.

[19] H. T. Hayvaci, A. De Maio, D. Erricolo, "Diversity in receiving strategies based on time-delay analysis in the presence of multipath," *2011 IEEE International Symposium on Antennas and Propagation and USNC/URSI National Radio Science Meeting*, Spokane, Washington, USA, July 3-8, 2011.

[20] H. T. Hayvaci, A. De Maio, D. Erricolo, "Performance analysis of diverse GLRT detectors in the presence of multipath, *Radar Conference (RADAR), 2012 IEEE*, 7-11 May 2012.

[21] C. Beard, I. Katz, L. Spetner, "Phenomenological vector model of microwave reflection from the ocean, *IRE Trans. Antennas Propag.*, vol.4, no.2, pp.162-167, April 1956.

[22] C. Beard, "Coherent and incoherent scattering of microwaves from the ocean, *IRE Trans. Antennas Propag.*, vol.9, no.5, pp.470-483, September 1961.

[23] D. Erricolo and P.L.E. Uslenghi, "Two-dimensional simulator for propagation in urban environments," *IEEE Trans. Vehicular Technology*, vol. 50, no. 4, pp. 1158-1168, July 2001.

[24] D. Erricolo, G. D'Elia, and P.L.E. Uslenghi, "Measurements on scaled models of urban environments and comparisons with ray-tracing propagation simulation," *IEEE Trans. Antennas Propag.*, vol. 50, no. 5, pp. 727–735, May 2002.

[25] D. Erricolo, U. G. Crovella, and P.L.E. Uslenghi, "Time-domain analysis of measurements on scaled urban models with comparisons to ray-tracing propagation simulation," *IEEE Trans. Antennas Propag.*, vol. 50, no. 5, pp. 736–741, May 2002.

[26] E. Conte, A. De Maio, and C. Galdi, "Signal detection in compound-gaussian noise: Neyman-Pearson and CFAR detectors, *IEEE Trans. Signal Processing*, vol. 48, no. 2, pp. 419–428, Feb 2000.

[27] H. L. Van Trees, *Detection, Estimation and Modulation Theory*, vol 1, New York: John Wiley & Sons, 2001.

[28] S. M. Kay, *Fundamentals of Statistical Signal Processing, Detection Theory*, vol 2, New Jersey: Prentice Hall, 1998.

[29] H. T. Hayvaci, P. Setlur, N. Devroye, D. Erricolo, "Maximum Likelihood Time Delay Estimation and Cramér-Rao Bounds for Multipath Exploitation," *Radar Conference (RADAR), 2012 IEEE*, 7-11 May 2012.

[30] S. M. Kay, *Fundamentals of Statistical Signal Processing, Estimation Theory*, vol 1, New Jersey: Prentice Hall, 1993.

[31] J. P. Imhof, "Computing the Distribution of Quadratic Forms in Normal Variables," *Biometrika*, vol. 48, no. 3/4, 417-426, Dec 1961.

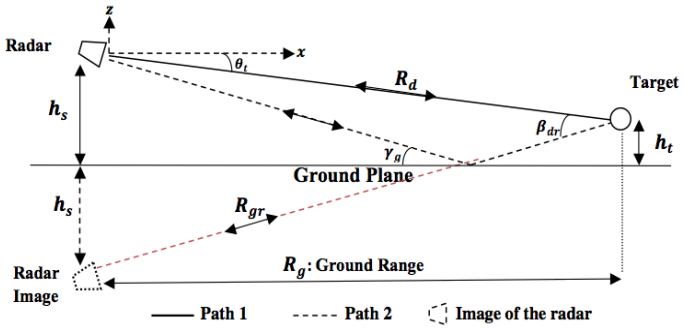

Fig. 1. Geometry of the problem: Radar-Target over a Ground Plane.

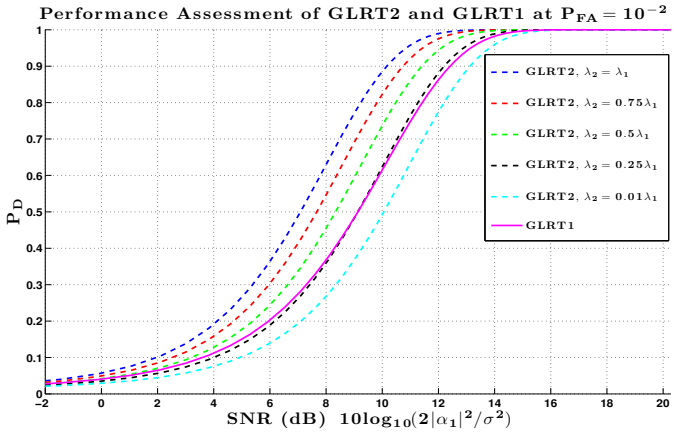

Fig. 2. Detection performance of detectors GLRT2 (21) with $P_{D_{\mathbf{GLRT2}}}$ (33), and GLRT1 (15) with $P_{D_{\mathbf{GLRT1}}}$ (27) for various values of the ratio $\frac{\lambda_2}{\lambda_1} = \frac{|\alpha_2|^2}{|\alpha_1|^2}$.

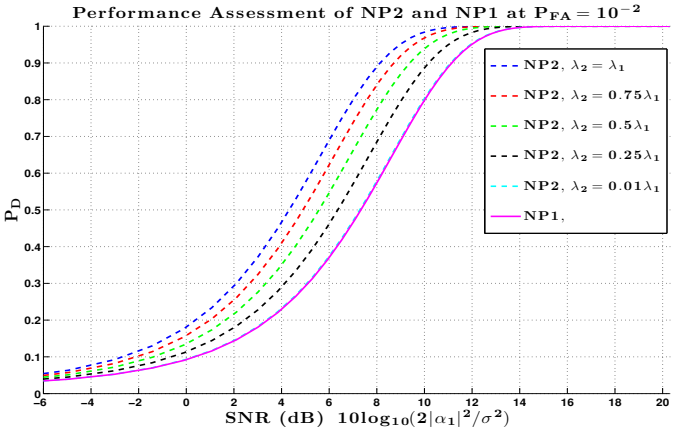

Fig. 3. Detection performance of detectors NP2 (19) with $P_{D_{\mathbf{NP2}}}$ (30) and NP1 (14) with $P_{D_{\mathbf{NP1}}}$ (24) for various values of the ratio $\frac{\lambda_2}{\lambda_1} = \frac{|\alpha_2|^2}{|\alpha_1|^2}$.

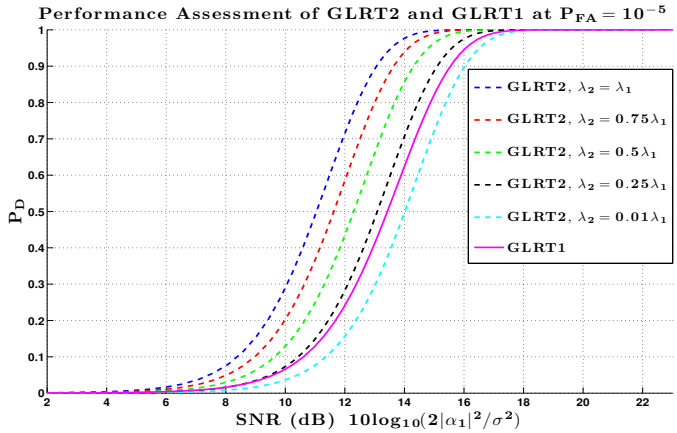

Fig. 4. Detection performance of detectors GLRT2 (21) with $P_{D_{\mathbf{GLRT2}}}$ (33) and GLRT1 (15) with $P_{D_{\mathbf{GLRT1}}}$ (27), for various values of the ratio $\frac{\lambda_2}{\lambda_1} = \frac{|\alpha_2|^2}{|\alpha_1|^2}$.

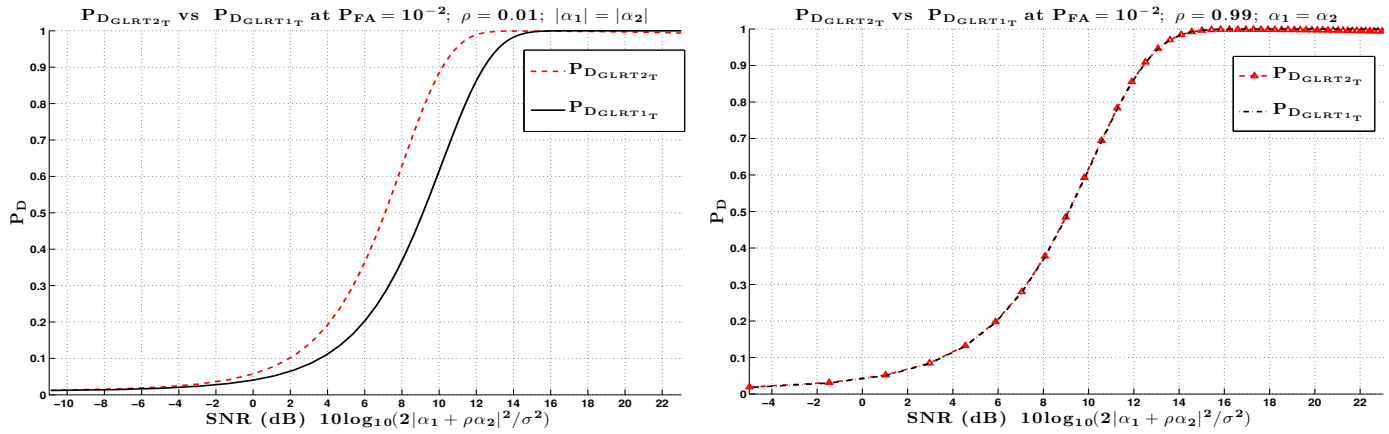

(a) (b)

Fig. 5. $P_{D_{\mathbf{GLRT2_T}}}$ vs $P_{D_{\mathbf{GLRT1_T}}}$ when (a) $\rho = 0.01$ and (b) $\rho = 0.99$.

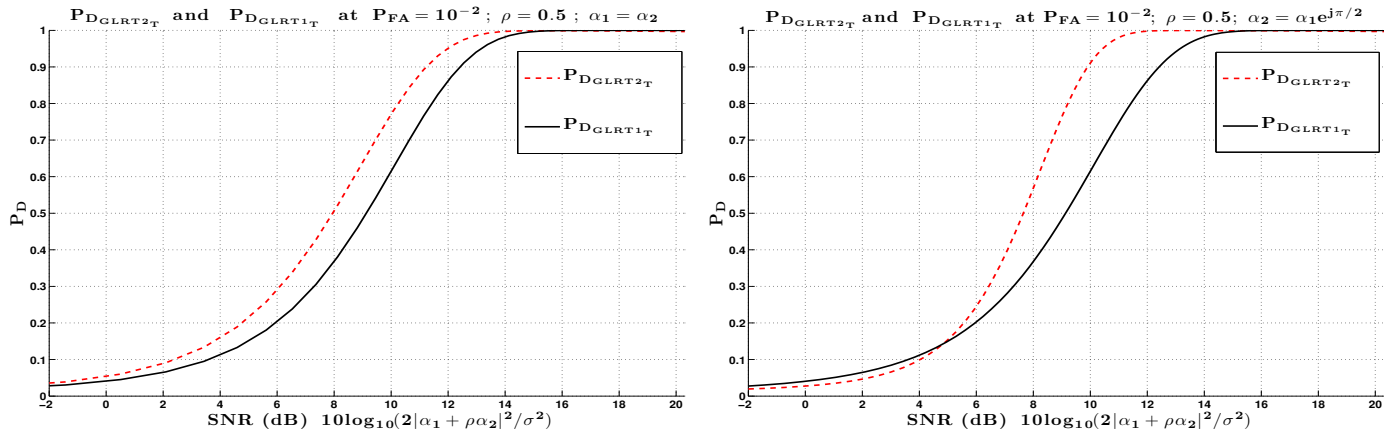

(a) (b)

Fig. 6. $P_{D_{\mathbf{GLRT2_T}}}$ vs $P_{D_{\mathbf{GLRT1_T}}}$ when $\rho = 0.5$: (a) α_1 and α_2 are in-phase; (b) α_1 and α_2 are out-of-phase.

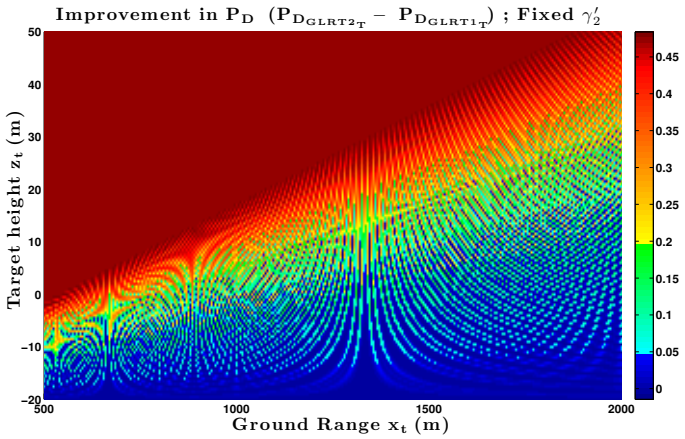

Fig. 7. Improvement in the target probability of detection of GLRT2 relative to GLRT1 at any hypothetical target location in the multipath environment.